IEEE Access
Multidisciplinary | Rapid Review | Open Access Journal

Received 7 December 2023, accepted 19 December 2023, date of publication 25 December 2023,
date of current version 12 January 2024.

Digital Object Identifier 10.1109/ACCESS.2023.3347500

RESEARCH ARTICLE

A Risk-Based Decision-Making Process for Autonomous Trains Using POMDP: Case of the Anti-Collision Function

MOHAMMED CHELOUATI[1], ABDERRAOUF BOUSSIF[2], JULIE BEUGIN[2], AND EL-MILOUDI EL-KOURSI[2]

[1]Technological Research Institute Railenium, 59300 Valenciennes, France
[2]COSYS-ESTAS, Gustave Eiffel University, 59650 Villeneuve d'Ascq, France

Corresponding author: Mohammed Chelouati (mohammed.chelouati@railenium.eu)

This work was supported by the "Train Autonome—Service Voyageurs" project (Autonomous Train—Passengers Service), co-financed by Société Nationale des Chemins de Fer français (SNCF) and Railenium, and involving the partners Alstom, Bosch, Spirops, and Thales.

ABSTRACT As the railway domain progresses towards autonomy, maintaining safety at levels comparable to human-operated systems is a crucial challenge. Autonomous trains require advanced systems capable of real-time risk assessment and decision-making, a task traditionally managed by human situational awareness. This paper introduces a novel risk-based decision-making approach for autonomous trains, using Partially Observable Markov Decision Processes (POMDPs) for continuous monitoring and evaluation of environmental collision risks. By consistently maintaining an acceptable risk level through ongoing risk estimation (in terms of occurrence probability and severity degree), the approach supports the decision-making capabilities of the autonomous driving system in autonomous trains, enabling safe and informed decisions despite the uncertainties in the train's operational state and environmental conditions. The approach's relevance and effectiveness are illustrated through its application in an anti-collision function for autonomous trains.

INDEX TERMS Autonomous train, dynamic risk assessment, Markov decision process, safety assurance.

I. INTRODUCTION

The emergence of autonomous trains is expected to introduce significant changes in the transportation industry [1]. The growing interest in this technology reflects its potential to transform railway systems and operations. This shift is not merely theoretical, but is being actively pursued in various parts of the world. In early 2016, the Direction of Railway Systems[1] (SNCF) in France initiated a technological program called Tech4Rail. This ambitious initiative aimed to lay the foundation for future railway systems and to prepare for the introduction of safe autonomous and semi-autonomous train operations. Working collaboratively with the Autonomous Train program of the Railenium Technological Research Institute,[2] alongside various industrial and academic partners, two consortia have been formed. These consortia have spearheaded three major projects, each with distinct objectives [1], [2]: (1) the autonomous freight train; (2) the autonomous passenger train and (3) the remote driving train. While these projects encompass numerous engineering research challenges, they primarily focus on the exploration of Artificial Intelligence (AI) techniques [3], [4], [5] in perception [6], [7], control and decision-making functions [8]. Additional focus areas include human-machine cooperation [9], societal acceptance of autonomous technologies [10], as well as risk assessment[3] and safety demonstration [12], [13], [14].

The French initiative is part of a global movement to advance autonomous transportation systems. For example,

The associate editor coordinating the review of this manuscript and approving it for publication was Jesus Felez.

[1]https://www.sncf.com/fr

[2]https://railenium.eu

[3]Risk assessment is the overall process comprising a risk analysis and a risk evaluation [11].

the Enable-S3 [15] project seeks to validate autonomous systems across different sectors, including rail, through innovative testing methodologies. Similarly, the SAFEDMI project [16] is working to improve the safety of railway traffic management by developing a more robust interface for train operators. In Germany, the SafeTrain project [17] is developing an integrated safety concept for autonomous trains. This project uses digital technologies and AI to enhance safety, including the development of obstacle detection systems and decision-making algorithms. In the UK, the AutoDrive project [18] is another important initiative. It aims to speed up the adoption of automated train operations on the UK rail network, focusing on how automation can enhance capacity, reliability, and safety. Recently, the Europe's Rail Joint Undertaking[4] has launched a 160M project, called R2DATO - Rail to Digital automated up to autonomous train operation.[5] Gathering the main European Railway companies, R2DATO aims to leverage digitalization and automation (up to full autonomous) to enhance the capacity of existing rail networks, intending to deliver Automated Train Operation (ATO) and advanced digital technologies by 2025.

According to safety standards and regulations, the safety level of emerging railway systems, such as autonomous trains, should be maintained, and if possible improved [12]. Indeed, the assurance of this safety level is intrinsically related to the train's capacity to perform all the operational tasks safely. Among these tasks, a key component function is the train's ability to understand its environment and react accordingly. Concretely, the on-board Autonomous Driving System (ADS) should continuously explore and interpret the surrounding environment and operational conditions in order to adapt its operation in real-time, ensuring the avoidance of any hazardous situation [19].

In conventional trains (operated by human drivers), safety demonstration and risk assessment processes form integral parts of the design and development phases. In fact, the risk assessment process of such systems is carried out by assuming the presence of a human operator on-board the train. Indeed, in addition to driving tasks, the driver performs a *dynamic risk assessment* during the train operations, informed by the train's state of health and capabilities. This dynamic risk assessment[6] (DRA) includes the detection and identification of potential obstacles, followed by the human decision-making that ensures, in case of unexpected obstacles, the safety of the train and its passengers [19], [20]. When it comes to autonomous trains, the ADS has to perform a similar process. Concretely, the ADS must demonstrate the ability to safely execute its functions across all situations and operational conditions. To assure this mission, the ADS should incorporate real-time and dynamic risk assessment, while the real-time risk assessment is defined as *"the process of assessing the current and immediate risk level."* capabilities within its decision-making process. These capabilities play a pivotal role in enhancing basic functions, such as obstacle detection, while also providing a solid foundation for the development of more advanced features, such as the anti-collision system [21], [22]. Consequently, the ADS, endowed with DRA and additional safety features, should ensure safer and more efficient autonomous train operations [23].

One of the challenges so that the ADS to be able to realize safety functions is the presence of potential uncertainties related to the perception system (sensors, and AI algorithms) and the environmental conditions [24], [25]. Indeed, the non-reliable received information could lead to missed detection and, at worst, to catastrophic consequences. Arising from this challenge is the need for a comprehensive and robust decision-making process capable of taking into account and handling uncertainties. This process should be designed to examine sensors' information, taking into account the potential for inaccuracies, and react accordingly.

In response to these challenges, the contribution of the paper consists in developing a risk-based[7] decision-making process for the anti-collision function of autonomous trains. The proposed process is able to account for the inherent uncertainty associated with the train state and the wide range of operational and environmental conditions, by using Partially Observable Markov Decision Processes (POMDPs).

The developed approach is based on continuously updated system information, including those related to the risk of collisions with potential obstacles. Notice that the risk is defined as *a combination of expected frequency of loss and the expected degree of severity of that loss* [11]. Handling risk-related information in operational-related data can lead to a well-balanced trade-off between the safety of the system and its availability.

This work is organized as follows. Section II presents the related works addressing uncertainties in decision-making processes of autonomous systems. Additionally, the benefits of integrating POMDPs in such processes for risk control are discussed. In Section III, the problem statement related to the anti-collision function for the autonomous train is detailed, along with the way to structure the associated risk data needed to complete the DRA task. Furthermore, the methodology of the proposed solution is described in Section IV, including the definition of the POMDP model, and the proposed risk model. The results of the experiments are presented in Section V. Finally, Section VI provides some concluding remarks and highlights some perspectives for future research.

[4]https://rail-research.europa.eu/

[5]https://www.uitp.org/projects/r2dato/

[6]Dynamic risk assessment is a method that continuously updates estimated risk of a deteriorating process according to the performance of the control system, safety barriers, inspection and maintenance activities, the human factor and procedures [19].

[7]A risk-based approach is the process of ensuring the safety of products, processes and systems through consideration of the hazards and their consequent risks [11].

II. TOWARD THE USE OF POMDPS IN ADS

First of all, the objectives of functions and tasks of the autonomous train ADS, especially those related to its decision-making process, are reminded. Then, some research works dealing with uncertainties in decision-making processes, whatever the terrestrial transportation system, are reviewed, including the different existing techniques. The focus is placed on one of them, POMDPs, given their proven benefits and their possible adaptation to dynamic risk assessment, as demonstrated in this section. The principles of POMDPs are not detailed here, as they will be presented in Section IV.

A. OBJECTIVES OF FUNCTIONS AND TASKS OF THE ADS

To ensure safe train operations in an open environment, the autonomous train must perform a variety of functions, including managing train states, avoiding collisions with obstacles on the track, and other critical functions. All of these functions are carried out by the ADS [1], which refers to *the set of hardware and software capable of performing the entire Dynamic Driving Task (DDT) on a sustained basis*, according to [26].

In the case of autonomous trains, the DDT has to include traditional train driver tasks such as environment perception, situation awareness, dynamic risk assessment, decision-making, and control tasks. In this subsection, among these tasks, we focus on the decision-making processes in autonomous trains.

Figure 1 depicts the essential components of the ADS in an autonomous train. In fact, the decision-making unit receives all the necessary information from the perception unit, computes main (operational and safety) indicators, and takes adequate actions The dynamic risk assessment task has to form the safety basis (via risk model) of the train decision-making process. Depending on the evaluated risk level, the ADS should then decide on an action plan. It could choose, for example, to accelerate or maintain speed to meet the speed profile of the train when no obstacle is present on the horizon, decelerate if a potential obstacle is detected at a safe distance, or initiate an emergency braking procedure if an immediate collision risk is identified.

Notice that, in railway standards, particularly as outlined in EN 50126, a 'risk model' is the comprehensive framework designed for the systematic identification, assessment, and management of risks in railway operations. The risk model's main objective is quantifying the likelihood and severity of potential hazardous events, evaluating the effectiveness of existing safety measures, and determining the need for additional risk mitigations. The model typically (for conventional railway systems) encompasses the identification of hazards, the risk analysis (including frequency and consequences of hazardous events), and the evaluation of risk against predefined acceptability criteria. On the other hand, risk models for autonomous trains should incorporate real-time information. This allows for an adaptive response to changing environmental conditions and operational scenarios. Using advanced algorithms, the model evaluates risk levels continuously, considering both historical data and real-time sensory inputs.

B. HANDLING UNCERTAINTIES IN DECISION-MAKING PROCESSES

Addressing uncertainties in decision-making for autonomous systems had emerged as a central research focus, identifying key problematics such as sensor fusion [27], [28], perception under varying environmental conditions [29], [30], and dynamic system state evaluation [31], [32]. These challenges are critical as they directly impact the safety and reliability of autonomous operations. Sensor fusion is particularly essential for ensuring comprehensive perception [33], as it integrates data from multiple sensors to form a coherent understanding of the environment, compensating for the limitations of individual sensors [34]. The literature reveals that environmental conditions significantly affect the perception accuracy [35], where factors such as lighting, weather, and obstructions can lead to uncertainties in detecting and classifying objects [36]. Moreover, maintaining an accurate system state is imperative, as it forms the basis for all subsequent decisions [37]. Variability in operational conditions and the need for real-time responsiveness necessitate robust frameworks and methodologies capable of adapting to sudden changes and predicting future states.

In fact, several research works in the literature focus on robust decision-making methodologies capable of taking into account various types of uncertainties. For instance, Bayesian Networks (BN) provides a graphical model to comprehend the probabilistic relationship among a set of variables and manage uncertain information [38], while Dynamic Bayesian Networks (DBN) extend this capability by handling temporal dependencies between variables [39]. Moreover, decision trees offer a simple and intuitive method to model decisions and their possible consequences, including outcomes, resource costs, and utility [40]. Lastly, Reinforcement Learning (RL) offers an interactive approach to learning an optimal policy for direct trial-and-error interaction with a dynamic environment [41], [42], [43]. However, among these methodologies, Partially Observable Markov Decision Processes (POMDPs) have gained significant attention in the realm of autonomous systems as described below.

C. BENEFITS OF POMDP IN DECISION-MAKING PROCESSES

POMDPs have several advantages when dealing with the decision-making process. Firstly, POMDPs explicitly account for the uncertainty in both the system's state and the observations. This feature is essential in autonomous systems where sensor readings may not always be reliable or complete, and the actual state of the environment is hard-to-specify and hard-to-predict. Secondly, unlike methodologies such as decision trees that operate on discrete models, POMDPs can handle continuous states, actions, and

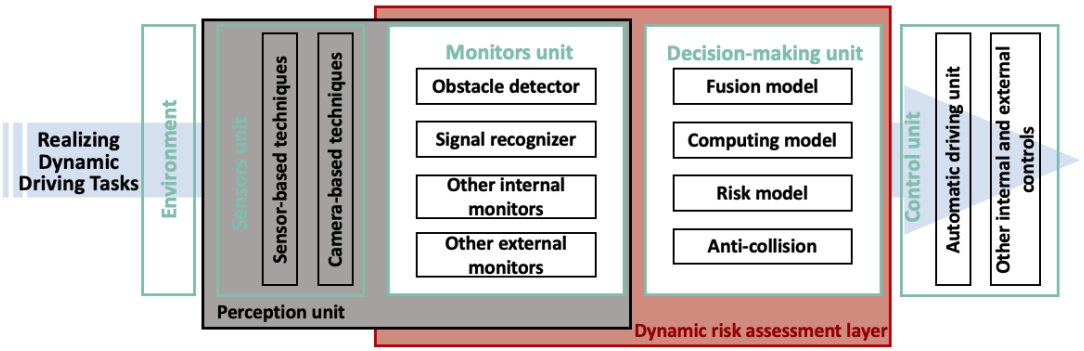

FIGURE 1. A simplified architecture of the ADS with a main focus on the DRA layer strengthening the decision-making task.

observation spaces. This is particularly useful for autonomous systems where the environment is often better represented as a continuous space, such as the relative positions and speeds of vehicles [44]. Finally, while the RL is also a powerful tool for decision-making under uncertainty, it typically requires a large number of trials to learn the optimal policy, which may not always be feasible or safe in critical applications like autonomous trains. On the other hand, POMDPs offer a model-based approach that allows efficient policy computation based on the system's model.

In addition to their capability to address uncertainty, POMDPs can also model both the stochasticity in environment transitions and imperfect sensory information [45]. This dual capability becomes vital when dealing with real-time sensor data that inherently contains observational noise and varying environmental states [46].

A number of studies have focused on the use of POMDPs for various tasks related to the decision-making process, including dynamic probabilistic risk assessment [47], cruise control of high-speed trains [48], collision avoidance in uncertain environments [49], and behavior planning for autonomous vehicles [45]. In the field of robotics, POMDPs have also been applied for fault management in autonomous underwater vehicles [50]. A survey by [51] provided a comprehensive overview of the use of POMDPs in robotics.

The literature also provides a range of algorithms and techniques for solving POMDPs, including online solvers [52], Monte-Carlo planning [53], and regularization methods [54]. In addition, various tools and frameworks have been developed to aid in the modeling and analysis of autonomous system behavior using POMDPs, such as TAPIR [55], an online approximating and adapting software toolkit [56], and the Expandable-Partially Observable Markov Decision-Process Framework [45]. Equivalently, the use of Deep Reinforcement Learning (DRL) in combination with POMDPs has been gaining popularity in recent years. For example, [57] explored the recent advances in DRL applications for solving POMDP problems in various fields, including transportation, industries, communication, and networking.

The above-mentioned papers highlight the various methods and techniques that have been developed to solve POMDPs in real-time and address the challenges of uncertain environments and dynamic parameters. Therefore, by using POMDPs, autonomous systems can make informed decisions that balance the trade-off between safety and efficiency (or even comfort), providing an important step toward the widespread adoption of autonomous systems.

We will now emphasize the central role that decision-making plays in ensuring the safety of autonomous trains by focusing in the following on one of its main functions: the anti-collision function.

III. PROBLEM STATEMENT RELATED TO ANTI-COLLISION FUNCTION

This section first provides a description of the anti-collision function, which is the focal point of the works described in this paper. Then, as explained before, the dynamic risk assessment (DRA) task has to be performed interdependently with the decision-making task. However, for assessing risk, having risk profile information is a prerequisite. Structuring such information is the output of the DRA framework proposed by the authors in [8]. This framework is revisited in this section, along with its application to the anti-collision function. In fact, obtaining structured risk information make it possible to provide inputs of our risk-based decision-making methodology using POMDP, which is described in the next section.

A. OBJECTIVES OF THE ANTI-COLLISION FUNCTION

The anti-collision function represents the train capacity to detect and react appropriately and safely to any potential obstacles that could instigate a collision. Notice that the obstacles to be considered are physical entities, such as other trains, vehicles, individuals, trees, and so on. It is essential for an autonomous train to be outfitted with the necessary sensors and algorithms to accurately identify the nature of an obstacle, and estimate its distance from the train and its trajectory, in order to compute and evaluate the associated risk. To realize the anti-collision function, the ADS monitors the operational state of the train and its surrounding environment, constantly scanning for potential obstacles.

Figure 2[8] illustrates a scenario where an autonomous train is approaching an intersection point in its track where the rail of another train merges. This is a potential area of conflict that the train's ADS recognizes and reacts to in a safer manner. Furthermore, on the horizon, a car road intersects the railway track, indicating a level-crossing scenario. A few individuals, along with their animals, are seen near the crossing, preparing to cross or possibly cross the railway track. This adds another layer of complexity to the scene, and the train's ADS must be capable of reacting to any potential obstacle and making decisions ensuring an acceptable safety level.

Moreover, the presence of trees alongside the rails is not merely an environmental feature in the figure. It signifies another set of potential risks, such as the danger of a fire, or the possibility of animals wandering onto the tracks from the forested areas. In such complex and unpredictable scenarios, the train's anti-collision function serves as the backbone, ensuring the safety of the autonomous train. It needs to efficiently process the potential risks arising from different aspects of the scenario (e.g., another train, humans and animals near the level crossing, cars, potential forest threats; etc.). The anti-collision function objective is not just to detect and identify these threats, but also to measure the level of risk associated with each one so that the decision can be made based on the most updated and accurate risk information.

FIGURE 2. Generic illustration of the anti-collision function.

Figure 2 serves as a reminder of the vast array of potential risks that an autonomous train might face, and how a robust, dynamic, and real-time risk assessment based on the anti-collision function can play a critical role in ensuring the safe operation of the train.

[8]This figure was generated using an AI-based image generation tool.

B. DRA TASK INHERENT TO THE ANTI-COLLISION FUNCTION

Given the uncertainties associated with real-world environments and sensor information, the observations help to form an *uncertainty estimation*. This estimation is a probabilistic representation of the current situation of the train, summarizing possible states of the train and its surroundings. Once the uncertainty estimation is established, the risk assessment inherent to the anti-collision function should be carried out. This refers to the DRA task, which has to be performed by the ADS to evaluate and update the risks associated with the current state of the train, the environment, and the available actions the train might take. This assessment is based on uncertainty estimation, considering both the likelihood and potential consequences of a collision. In addition, the uncertainty estimation plays an important role in establishing the risk profile, as it provides the probabilistic basis from which potential hazardous scenarios and their associated risks are assessed, and classified within the risk profile.

Figure 3 shows an illustrative scenario involving an autonomous train and a potential obstacle in its track. Different control actions are available for the train, in response to the surroundings and with respect to the criticality of the evaluated risks, namely, accelerating, maintaining the current speed, and various types of braking. In Figure 3, the obstacle is located at a certain distance on the track of the train. With respect to the distance from the train, three zones are considered: warning, emergency, and critical zones. The *warning* zone (in yellow color) indicates a distance from where no immediate action is needed (i.e., the obstacle is so far or not detected yet). The *emergency* zone (in orange color) signifies a cautionary distance from where the train may need to adjust its speed or brake in order to avoid a collision. Finally, the *critical* zone (in red color) signifies that the presence of an obstacle can lead to a collision (i.e., in this zone, the obstacle is considered close to the train, and even with an emergency braking the risk of collision is high). The associated risk level, represented on the vertical axis with a scale between 0 and 1, is estimated according to the distance to the obstacle. Obviously, the closer the obstacle is to the train, the higher the risk level is. The threshold to reach the unacceptable risk level (visualized in the figure by the intersection between the blue dashed line with the vertical axis) is crossed when the train crosses the *critical* zone.

Note that, the DRA task must not only lead to a safety reaction of the ADS when a collision risk is identified, but also learn from every decision made. The consequences of each decision have to be monitored and analyzed to understand the effectiveness of the actions taken. This feedback loop allows the system to continuously adapt and evolve, improving its performance over time. Therefore, the anti-collision function, performed by the DRA, acts as a dynamic learning and protection layer, ensuring a higher level of safety in the operation of autonomous trains.

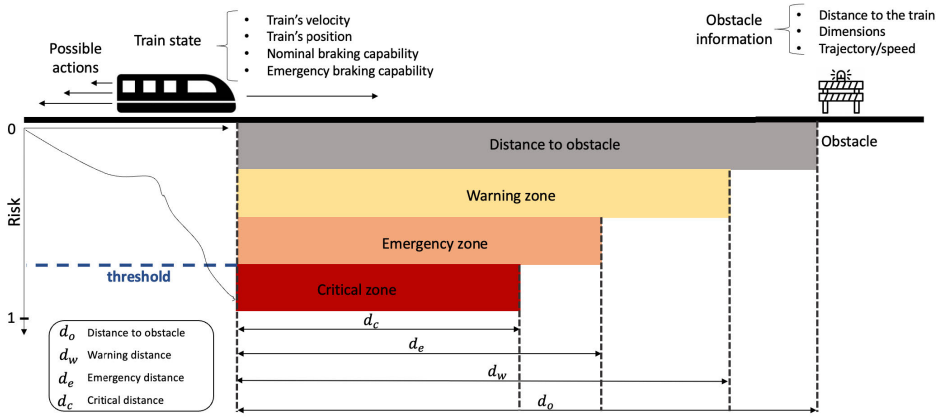

FIGURE 3. Illustrative representation of the anti-collision function.

For structuring the risk profile needed in the DRA, the framework described in [8] is now presented and applied to the anti-collision function.

C. STRUCTURING RISK PROFILES WITH THE DRA FRAMEWORK

The proposed framework provides a structured approach to decision-making, taking into account the train state uncertainty and the perception of the environment. The DRA framework is designed to take into account the various factors that influence the decision-making process (cf. Figure 4). This includes the train's speed, the distance to the obstacle, and the perception of the environment, among other internal and external factors.

This framework enables the ADS to perform a real-time evaluation and prediction of potentially hazardous situations by estimating their occurrence probabilities and severity. It exploits not only the information collected from the perception module but also translates this information into an actionable risk profile.[9] This profile then guides the decision-making process to efficiently determine the appropriate and safe actions necessary to avoid or mitigate the impact of hazards. Therefore, the integration of risk profiles into a DRA framework for autonomous trains allows for the real-time management and mitigation of risks, thereby improving overall safety in autonomous train operations.

In the present paper, our focus is on the Understanding & Prediction and Decision-making modules in the case of the anti-collision function. The Understanding & Prediction module utilizes the information provided by the Perception module to create and continually update an integrated real-time model that represents the system environment and its states. This model is subsequently utilized for run-time decision-making. From the perspective of DRA, this module enables the computation of a current risk estimate and the prediction of potential railway hazards. Subsequently, this risk estimate is evaluated through the risk model. This risk model for anti-collision purposes integrates both historical data, which reflects past system performance and incidents, with real-time sensor information to enhance the accuracy of potential collision predictions. Moreover, it evaluates several parameters, such as the train's current speed, position, and braking capabilities as well as the positions and velocities of detected obstacles. By continuously updating these parameters in real-time, the model is able to adjust and update the risk estimates associated with each potential action and thus assists in selecting the safest action for the autonomous train. Based on a comprehensive evaluation of the risk assessment parameters, the following section outlines the POMDP-based methodology developed to effectively address the safety challenges of autonomous train operations.

[9] According to [58], "*outcome, likelihood, significance, causal scenario, and population affected [are factors that] determine the risk profile.*"

IV. METHODOLOGY

In this section, we first recall the preliminary definitions and notions of POMDP, and then, we describe the different components of the POMDP model for the train's anti-collision decision-making process.

A. POMDP DEFINITION

A POMDP is a probabilistic method that models the sequential process of a system under uncertainty. It is a generalization of Markov Decision Process to situations where the system state is partially unknown. Formally, a POMDP is a tuple $\langle S, A, O, T, Z, R, \gamma \rangle$, where S and A are the sets of states and actions, T is the transition function that defines the conditional probability P of moving from one state $s \in S$ to another state $s' \in S$ as a result of executing an action $a \in A$, i.e., $T(s, a, s') = P(s' \mid s, a)$. O is the observation space that defines the information received (from sensors) after the execution of an action. Z is the corresponding observation function that defines the conditional probability of observing a particular outcome $o \in O$ after executing an action $a \in A$ to reach to state $s' \in S$, i.e., $Z(o, a, s') = P(o \mid s', a)$. R is the reward function $R(s, a)$ that defines

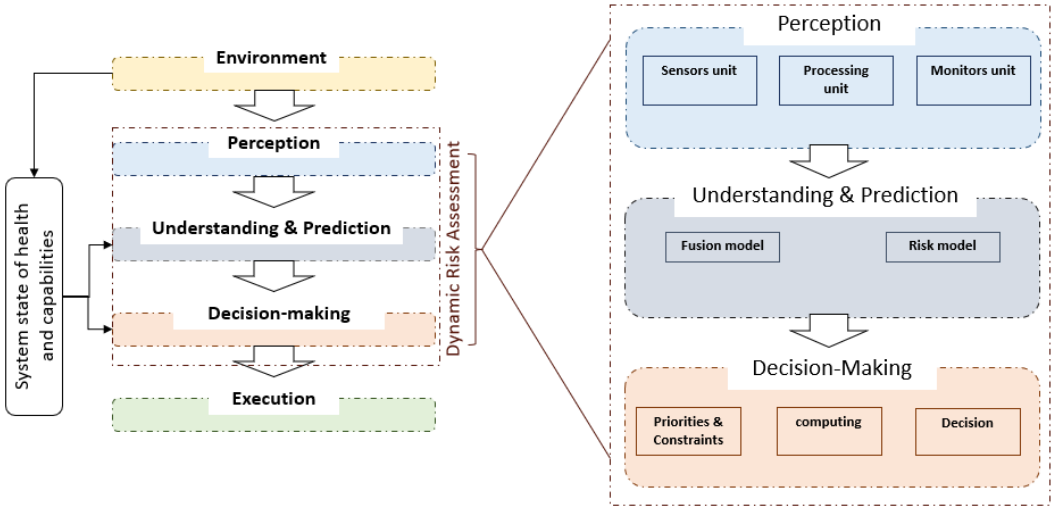

FIGURE 4. The autonomous train dynamic risk assessment framework.

the immediate reward received for being in a particular state $s \in S$ and taking a particular action $a \in A$. Finally, $\gamma \in [0, 1]$ is the discount factor that determines the relevance (or not) of future rewards.

In a POMDP, only partial and noisy knowledge of the system and its environment is considered; thus, a belief about the model states, known as a belief state $b(s)$, is continually inferred. The belief state is a probability distribution over the state space that reflects the degree of certainty maintained by the POMDP model about the current state of the system. Accordingly, a policy $\pi : B \rightarrow A$ is used as a mapping from the set of possible belief states to the set of actions, in order to determine the adequate action that should be taken.

Solving a POMDP involves finding the optimal policy π^* in terms of current action or finite sequence of actions to be executed in order to maximize (or optimize) the expected cumulative reward over time, taking into account the belief state. Formally,

$$\pi^*(b) = argmax_{a \in A}\{\sum_{s'} P(s' \mid b, a)[R(b, a, s') + \gamma . E[V^*(b')]]\} \quad (1)$$

To evaluate the potential reward of taking an action a and transitioning to state s', equation 1 considers the probability $P(s' \mid b, a)$ of transitioning to state s' given the current belief state b and the action a taken. It also accounts for the immediate reward $R(b, a, s')$ obtained from the action a in the belief state b and transitioning to state s'. Moreover, the equation considers the expected value (i.e., expected reward) of the optimal value function, $E[V^*(b')]$ for the next belief state b' resulting from the transition to state s'. This component accounts for the potential future rewards and outcomes taking action a.

The optimal policy in a POMDP can be computed using two main categories of solvers: *online* and *offline* solvers. These solvers differ in the way they find the optimal policy and the computational resources they require. Online solvers are designed to run in real-time and make decisions based on the current state of the system, while offline solvers are designed to run offline and make decisions based on historical data. The choice of the solver depends on the specific use case and the computational resources available.

B. POMDP MODELING OF THE TRAIN ANTI-COLLISION SYSTEM

1) TRAIN ANTI-COLLISION SYSTEM MODELING

The anti-collision system takes as input internal information regarding the train state, and external information about the environment. As explained in subsection III-C presenting the DRA framework, the internal inputs encompass sensor information about the train position and velocity (generally, provided by the localization and the speed measuring modules), as well as nominal and emergency braking (i.e., deceleration) capabilities, which can be transformed into the nominal and emergency distances to stop the train. On the other hand, external inputs refer to information about the surrounding obstacles (coming from the perception module), including their positions, dimensions, velocity, and intentions (for moving obstacles). The output of the system is the adequate control action (or sequence of actions) to be taken in order to avoid (when possible) any collision with the detected obstacle. Figure 5 presents a general view of the POMDP input-output structure used to implement the anti-collision function.

The continuous state-space of the POMDP model includes the state of the train and the states of the (eventually) surrounding obstacles. The state of the train s_T contains its position (x_T, y_T), its velocity v_T, and its orientation θ_T.

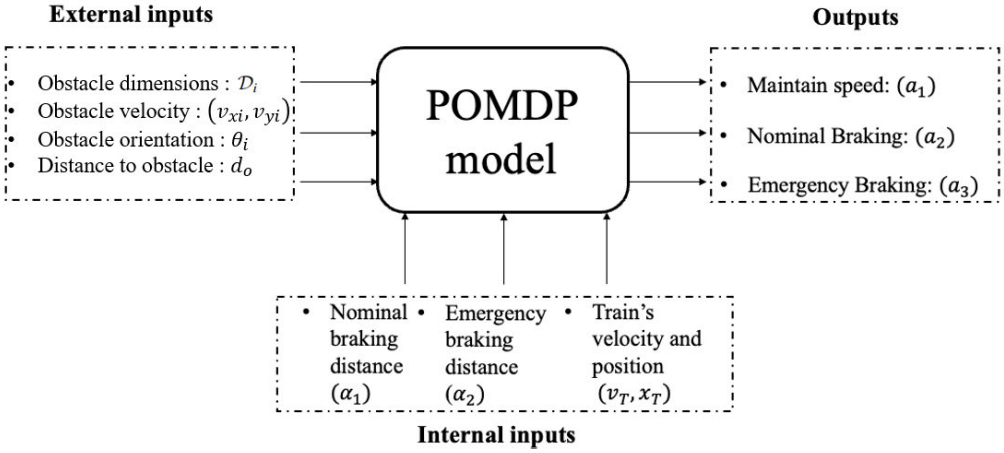

FIGURE 5. A generic illustration of the POMDP model.

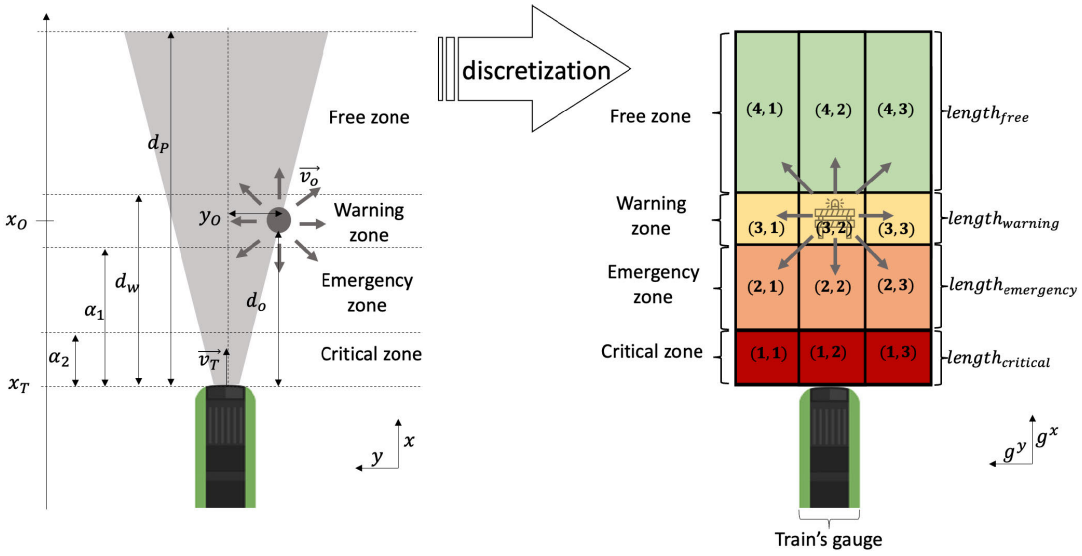

FIGURE 6. A generic spatial discretization of Cartesian plan into adaptive grid map for autonomous train navigation.

Similarly, the state of each obstacle s_i is composed of its position (x_i, y_i), its dimension $\mathcal{D}_i$, its instantaneous speed (v_{xi}, v_{yi}), and its orientation θ_i. It is worth noticing that such a formulation of the state space is performed on a global (or earth) coordinate system. An arbitrary point on the track is chosen as the origin of the coordinate system. Notice that several coordinate systems can be considered, as local and relative systems (See [59], [60] for more details).

While the continuous formulation of the state space is a faithful representation of the real system, it remains a very high-dimensional continuous space, which requires significant computation time and space to solve the model and find the adequate policy. Moreover, the existing algorithms to solve the continuous POMDP do not scale well when it comes to high-dimension continuous models. In order to remedy this issue, we consider in this paper a discrete POMDP with a discrete representation of state space, action space, and observation space.

2) MODELING THE DISCRETE STATE SPACE

The discretization of the state space is performed using a two-dimensional adaptive grid fixed to the head of the train. Thus, a local coordinate (ego-centric) system with the head of the train as system origin is considered. This means that instead of explicitly representing the positions of the obstacles as continuous variables within the model states, they are represented implicitly through several variables indicating the occupancy or not of the grid cells.

The positive x-axis is in the direction of train driving and the positive y-axis is directed to the left of the train head. Notice that the adaptive grid cell size is dependent on the tangible braking capabilities of the train, the presence of obstacles in (or alongside) the track, and the gauge of the train.

Figure 6 presents a two-part illustration from a real-world scenario of the adaptive grid map. The first part (*on the left of the figure*) shows a train moving along its track

with an obstacle appearing in its path, visualized using a global coordinate system. The second part of the illustration (*on the right of the figure*) depicts the adaptive grid map resulting from this discretization process. Furthermore, On the right side, the concept of discretization is shown. This is represented by a grid overlay on the track, with the grid cells numbered in parentheses. The cells are color-coded consistent with the zones described on the left: green for the free zone, yellow for the warning zone, orange for the emergency zone, and red for the critical zone. This grid represents a method for discretizing the continuous space around the train into manageable sections for the anti-collision system to evaluate risk more effectively. This discretization allows the transfer from the global coordinate system to an adaptive grid map. The lengths of each zone in this adaptive grid map are indicated on the right side of the grid as $length_{free}$, $length_{warning}$, $length_{emergnecy}$, and $length_{critical}$. The train's gauge, which is the width of the train or the tracks, is also noted at the bottom of the grid. In fact, figure 6 illustrates our approach to risk quantification, which, at first glance, emphasizes proximity and braking distances. However, the model's architecture inherently accommodates additional critical parameters. Lateral position is factored into the discretized grid map, where each cell corresponds to a specific lateral and longitudinal zone relative to the train, allowing us to account for the lateral positioning of obstacles. Moreover, obstacle velocity is incorporated into the risk assessment though dynamic cell updates that reflect the changing positions of obstacles over time. This enables the system to anticipate and react to moving obstacles, with a higher risk attribution for those with significant relative velocity towards the train.

The adaptive grid map is structured as a 12-cells grid, where each cell is defined based on the relative position of the obstacle (g^x, g^y), and its relative discrete orientation θ^d. Notice that the orientation of the obstacle is determined based on its velocity projections (v_x, v_y) (or its angular velocity ω_o), and represents the possible transitions to the eight surrounding grid cells.

Thus, the state set $\mathcal{S}$ can be expressed as follows:

$$\mathcal{S}=\begin{cases} g^x, & \text{with } g^x \in \{1,2,3,4\} \\ g^y, & \text{with } g^y \in \{1,2,3\} \\ \theta^d, & \text{with } \theta^d \in \{0, \frac{2\pi}{8}, \frac{4\pi}{8}, \frac{6\pi}{8}, \pi, \frac{10\pi}{8}, \frac{12\pi}{8}, \frac{14\pi}{8}\} \end{cases} \tag{2}$$

The variable g^x represents the discretization of the obstacle's position in the x-axis and can take four values $\{1, 2, 3, 4\}$, corresponding to the number of lines in the grid. The variable g^y represents the discretization of the obstacle's position in the y-axis and can take three values $\{1, 2, 3\}$, corresponding to the number of columns in the grid. Additionally, the variable θ^d represents the orientation of the obstacle and is discretized from a continuous space (from 0 to 2π) to eight discrete values $\{0, \frac{2\pi}{8}, \frac{4\pi}{8}, \frac{6\pi}{8}, \pi, \frac{10\pi}{8}, \frac{12\pi}{8}, \frac{14\pi}{8}\}$, representing the possible transitions to the eight surrounding cells. In fact, each unique combination of g^x, g^y, and θ^d represents a distinct state in the adaptive grid map, indicating the position and orientation of the obstacle (see Figure 6). With four possible values for g^x, three possible values for g^y, and eight possible values for θ^d, the total number of possible states in the adaptive grid map is $N_{\mathcal{S}} = 4 \times 3 \times 8 = 96$. These 96 states capture all the possible configurations of an obstacle within the adaptive grid map, enabling the POMDP model to effectively reason about its movement and potential interactions with the train in real-world scenarios.

In order to establish the size of each cell in the adaptive grid map, the next step of the discretization process is the definition of different zones (*Free*, *Warning*, *Emergency* and *Critical* zones). The boundaries of each zone are determined as functions of the nominal and emergency braking distances α_1 and α_2. In fact, the length of the cells in *Critical*, *Emergency*, and *Warning* zones are respectively equal to the emergency braking distance ($length_{critical} = \alpha_2$), the nominal braking distance ($length_{emergency} = \alpha_1 - \alpha_2$), the distance to the obstacle ($length_{warning} = d_w - \alpha_1$). Additionally, the length of the *free* zone cells is determined by the maximal perception distance (or the perception range) d_p of the autonomous train ($length_{free} = d_p - d_w$)). On the other hand, the width of all cells in the adaptive grid map is equal to the gauge of the train. Equation 3 shows the boundaries of each zone:

$$\begin{cases} Freezone = \{(g^x, g^y, \theta^d) \in \mathcal{S} \mid d_w < g^x \leq d_p\} \\ Warningzone = \{(g^x, g^y, \theta^d) \in \mathcal{S} \mid \alpha_1 < g^x \leq d_w\} \\ Emergencyzone = \{(g^x, g^y, \theta^d) \in \mathcal{S} \mid \alpha_2 < g^x \leq \alpha_1\} \\ Criticalzone = \{(g^x, g^y, \theta^d) \in \mathcal{S} \mid g^x \leq \alpha_2\} \end{cases} \tag{3}$$

These zones include the *Free* zone where no obstacle is detected, the *Warning* zone where an obstacle is present but can be avoided by a nominal braking, the *Emergency* zone where an obstacle can only be avoided by an emergency braking, and the *Critical* zone where an obstacle cannot be avoided, and a collision is imminent. In fact, in the adaptive grid map, each zone consists of three cells, resulting in a total of 12 cells.

From a safety perspective, if an obstacle is in one of the three cells within each zone, whatever the speed of the obstacle compared to the speed of the train, and knowing that its orientation is toward a lateral direction (i.e., $\theta^d = 0$ or π, meaning that the next obstacle state will remain in the same zone), the associated level of risks can be considered to be similar for the autonomous operation. If the obstacle orientation is forward (i.e., $\theta^d = \frac{2\pi}{8}$ or $\frac{4\pi}{8}$ or $\frac{6\pi}{8}$) or backward (i.e., $\theta^d = \frac{10\pi}{8}$ or $\frac{12\pi}{8}$ or $\frac{14\pi}{8}$), the risk will respectively decrease (only if $v_o \geq v_T$) or increases (only if $v_o > 0$). In order to define POMDP states with comprehensible risk levels, we adopt the following assumptions.

3) ASSUMPTIONS FOR DEFINING RISK LEVELS

It can be observed that most of the 96 states from the adaptive grid map can exhibit similar safety implications. In particular, the three cells within each zone can be related to a similar level of risk. In other words, multiple states might present an analogous level of risk for autonomous train operations. Such similarities across various states can be attributed to factors such as the immediate threat an obstacle can raise, the available reaction time for the train, and the potential consequences of inaction. Rather than distinguishing among these numerous states, which might only offer marginal differences in the actual risk, it appears to be more pragmatic and efficient to aggregate them based on their overall risk level. This not only streamlines the decision-making process but also ensures clarity in defining distinct risk levels.

Moreover, in the initial simulation setup described herein, it is assumed that obstacles detected by the autonomous train's perception unit are static (i.e., $v_o = 0$) in the immediate environment. This assumption simplifies the predictive aspect of obstacle movement and trajectory, allowing the decision-making process to forgo consideration of these dynamics. Consequently, the orientation (θ^d) of the obstacles is not taken into account when transitioning to discrete safety states. The focus is primarily on identifying obstacles and gauging their proximity to the train (i.e., the distance to obstacle d_o). In contrast, the second simulation setup advances this model by integrating the velocity of obstacles and their nature (i.e., static or dynamic). This not only reflects a more realistic operational scenario but also challenges the system to account for the additional complexity in its risk assessment and decision-making algorithms. Furthermore, developing two simulation setups highlights the adaptability of the approach, showcasing its capacity to integrate multiple factors, whether they are external factors related to obstacles or internal factors associated with the train itself.

Based on the outlined considerations, we have identified four discrete states. This delineation is not just a reduction, but a methodical classification and categorization based on the risk levels that several states in the adaptive grid map might be associated with. This structured approach provides a clear representation of collision risks, facilitating an efficient response by the autonomous train system to safety-critical situations. The specifics of these four states are detailed in Equation 4, as shown at the bottom of the page.

Finally, the state *Safe* indicates that no obstacle is detected in the train's surroundings. This situation applies to the *Free* zone, where the distance to obstacle $d_O \to \infty$. Conversely, the *ObstacleDetected* state signifies that an obstacle is located in the *Warning* zone. In this zone, the obstacle can be avoided by nominal braking. However, if the obstacle breaches the *Emergency* zone, the state switches to *AboutToCrash*. This state represents a significant risk that necessitates the immediate application of emergency braking to prevent a collision. Finally, the *Crash* state denotes the situation where the obstacle is located in the *Critical* zone, and a collision is inevitable despite any measures.

4) MODELING THE ACTION SPACE

The dynamic behavior of the train is mainly controlled by the continuous action of acceleration (and intrinsic deceleration and braking). To simplify the model, we consider a discretization of the acceleration space into three discrete values $\mathcal{A} = \{a_1, a_2, a_3\}$, which represent respectively: maintaining the speed, nominal braking, and emergency braking.

It is worthwhile noticing that, in the context of obstacle avoidance, the (positive) acceleration action can also be considered. This action is generally taken in the case of hazardous situations related to fires in the track or the presence of smoke in tunnels. In this study, such a kind of situation is not considered.

5) MODELING THE OBSERVATION SPACE

The observation space, denoted $\mathcal{O}$, is defined as the set of possible observations that the autonomous train can make at each time step. In fact, all observable variables constructing the observation space, such as train position and velocity, can be updated directly from sensor measurements. Noise in these sensor measurements can also be taken into account during observation and belief updates. In our case, the observation space comprises the obstacle's position in the adaptive grid map, represented by the variables g^x and g^y. This representation captures the relative location of the obstacle with respect to the train's position and enables the assessment of potential collision risks. Thus, two observations are defined in the following set:

$$\mathcal{O} = \begin{cases} g^x, & \text{with } g^x \in \{1, 2, 3, 4\} \\ g^y, & \text{with } g^y \in \{1, 2, 3\} \end{cases} \tag{5}$$

6) MODELING THE TRANSITION FUNCTION

Based on the probability distribution of the initial (or current) state of the model, at each step time δt, an action is taken and the probability distribution over the state space is updated according to the transition function model $T(s, a, s') = P(s' \mid s, a)$. The transition function depicts the dynamic

$$\mathcal{S} = \begin{Bmatrix} s_1 \\ s_2 \\ s_3 \\ s_4 \end{Bmatrix} = \begin{cases} \textit{Safe} & = \{(g^x, g^y, \theta^d) \mid g^x = 4, \forall\, g^y, \theta^d\}, \\ \textit{ObstacleDetected} & = \{(g^x, g^y, \theta^d) \mid g^x = 3, \forall\, g^y, \theta^d\}, \\ \textit{AboutToCrash} & = \{(g^x, g^y, \theta^d) \mid g^x = 2, \forall\, g^y, \theta^d\}, \\ \textit{Crash} & = \{(g^x, g^y, \theta^d) \mid g^x = 1, \forall\, g^y, \theta^d\} \end{cases} \tag{4}$$

behavior of the train and obstacles after each step time δt. We consider v_T, x_T, and a_{cc}^T being the train velocity, position, and acceleration respectively, with the time sample δt. The following equation shows the train's transition model (i.e., train's dynamics) in the global (or earth) coordinate system:

$$\begin{bmatrix} v_T(t+\delta t) \\ x_T(t+\delta t) \end{bmatrix} = \begin{bmatrix} 1 & 0 \\ \delta t & 1 \end{bmatrix} . \begin{bmatrix} v_T(t) \\ x_T(t) \end{bmatrix} + \begin{bmatrix} \delta t \\ \frac{\delta t^2}{2} \end{bmatrix} . a_{cc}^T(t) \quad (6)$$

Similarly, the obstacle's transition model (i.e., obstacle's dynamics) in the global coordinate system is described as follows:

$$\begin{bmatrix} v_o(t+\delta t) \\ x_o(t+\delta t) \end{bmatrix} = \begin{bmatrix} 1 & 0 \\ \delta t & 1 \end{bmatrix} . \begin{bmatrix} v_o(t) \\ x_o(t) \end{bmatrix} \quad (7)$$

Notice that in the case of the obstacle's transition model, the acceleration is not considered. In addition, we assume that the transitions are deterministic, and the obstacle remains static in time. The new distance to the obstacle d_o after a time step (i.e., the obstacle's transition model) in the global coordinate system is represented by the following equation:

$$d_o(t+\delta t) = d_o(t) - v_T(t).\delta t - a_{cc}^T(t).\frac{\delta t^2}{2} \quad (8)$$

However, the distance to the obstacle in the local coordinate system (adaptive grid map) is defined as follows:

$$d_o(t) = g_o^x(t) \quad (9)$$

7) MODELING OBSERVATION FUNCTION

The main objective of the observation function $Z(o|s,a)$, in this case, is to calculate the distance traveled by the train after a time step, in the global coordinate system. This distance allows keeping track of the new distance to the obstacle in each action selected from the action space.

$$d_T^{traveled}(t+\delta t) = v_T(t).\delta t + a_{cc}^T(t).\frac{\delta t^2}{2} \quad (10)$$

The new distance to the obstacle, after a time step, becomes:

$$d_0(t+\delta t) = d_0(t) - (v_T(t).\delta t + a_{cc}^T(t).\frac{\delta t^2}{2}) \quad (11)$$

Similarly, the orientation of the obstacle can be updated, at each time step δt, based on the obstacle's orientation at the previous time step and the obstacle's angular velocity ω_o. Thus:

$$\theta_{t+\delta t}^d = \theta^d(t) + \omega_o.\delta t \quad (12)$$

Notice that equation 12 assumes that the obstacle's angular velocity (ω_o) remains constant over the time step δt. This fits the assumption made previously that the obstacle remains static in the global coordinate system. In fact, the static obstacle's position in the global coordinate system corresponds to a constant angular velocity in the local (or relative) coordinate system (i.e., adaptive grid map).

8) REWARD FUNCTION

The reward function is in the form of costs (or negative rewards), assigned to each decision (action) made by the model within a specified state [59]. The role of the reward function is to encourage decisions that advance the system's goals, while imposing penalties on those that do not. Whilst the primary objective of the anti-collision system is to prevent train collisions, it remains desirable to consider other secondary objectives, such as respecting the timetable schedule, maintaining a smooth velocity, etc.

For the primary objective, negative rewards (i.e., penalties) are assigned to states that are considered unsafe, such as those that have a high probability of collision with an obstacle (e.g., the *Crash* state). By assigning higher negative rewards to riskier states, the ADS can be incentivized to take safer actions and avoid collisions. This reward adaptation according to risk embodies the risk model mentioned in section III. It can be updated in real-time as new information about the environment becomes available, allowing the system to continuously adapt to changing conditions and maintain a safe operation. Moreover, the reward function assigns numerical values to each state-action pair to simulate the desired behavior. In our case, the main objective of the system is to avoid when possible (i.e., minimize the risk of) the train collisions. Hence, we define an important penalty to the train to be in the *Crash* state (s_4), another penalty for the *AboutToCrash* state (s_3), and a reward for being in the *Safe* state (s_1). The reward function is represented by equation 13:

$$\mathcal{R}(s) = \begin{cases} 10, & \text{if state } s = s_1 \text{ (Positive Reward)} \\ -10, & \text{if state } s = s_2 \text{ (Minor Penalty)} \\ -100, & \text{if state } s = s_3 \text{ (Moderate Penalty)} \\ -1000, & \text{if state } s = s_4 \text{ (Severe Penalty)} \end{cases} \quad (13)$$

One important consideration when designing the risk model for the ADS is the trade-off between safety and efficiency. In particular, for states such as *ObstacleDetected* and *AboutToCrash* (i.e., s_2 and s_3), the reward function should balance the desire to avoid collisions with the need to maintain efficient driving behavior. Assigning overly negative rewards/penalties to these states may cause the system to become overly cautious and overly slow, which can lead to inefficient or impractical driving behavior. On the other hand, assigning insufficiently negative rewards (i.e., penalties) may lead to unsafe driving behavior, where the system takes risky actions in order to maintain high efficiency. Finding the right balance between safety and efficiency is a key challenge in designing the risk model for the autonomous driving system. For instance, we established the reward function as follows:

The method described in this section serves as the basic framework for conducting simulations and presenting the results in Section V.

V. SIMULATION AND RESULTS

In this section, we provide a detailed description of the experimental set-up, elaborate on the process of variable initialization, and present the simulation results.

The simulations established in this paper provide insights into the decision-making processes of the autonomous train, with a particular emphasis on ensuring safety and an effective anti-collision function. We present two simulation scenarios: the original, based on the POMDP model that takes only the distance to an obstacle as input, and an advanced setup that integrates the velocities and the nature of obstacles (i.e., static or dynamic obstacles). These simulations collectively offer a way to evaluate the system's performance under controlled yet realistic conditions, negating the risk and financial implications associated with real-world testing. This process' practical use includes essential components, each with an important role in the simulation process:

A. PERCEIVED STATE

The perceived state is crucial for connecting the real and simulated environments. In fact, observed distance and perceived obstacles in this simulation are subject to Gaussian noise, emulating uncertainties inherent to real-world sensing. The train's next action is decided based on the perceived state, derived from these noisy observations, and not from the actual state.

B. OBSTACLE GENERATION FUNCTION

In the simulation model used in this paper, obstacles are generated stochastically in the train's path. The appearance of an obstacle is determined by a random function, occurring approximately 20% of the time, with the distance to a new obstacle drawn from a uniform distribution. This obstacle-generation process introduces diversity into the simulation and allows testing of the reliability of the train's decision-making in various situations. Moreover, obstacles are generated, following a uniform distribution, between the mean of the nominal and emergency braking distances (α_1 and α_2) and 50 meters beyond this mean respectively. This ensures that the obstacles are generated within a reasonable range of distances where the autonomous train could have a fair chance to detect them and react appropriately.

This choice of obstacle generation provides a balance between the extremes of having all obstacles too close, which might not provide sufficient reaction time for the train, and having them too far, which might not pose any real danger or challenge to the train's ADS.

C. BELIEF UPDATER

The belief updater is a critical component of the model. It retains a distribution over potential states the autonomous train may occupy, integrating the actual state, perceived state, and actions taken. The belief state is generated for each time step, playing an essential role in handling uncertainties in the system and enabling more robust decision-making. The belief update equation is given by:

$$b'(s') = \eta \cdot P(o|s', a) \cdot \sum_{s \in \mathcal{S}} P(s'|s, a) \cdot b(s) \tag{14}$$

In equation 14, η is the normalization constant to ensure that the updated belief state b' is a valid probability distribution (i.e., sums to 1 over all states). $b(s)$ and $b'(s)$ are the probability of being, respectively, in the current state belief state s and the updated belief state s'.

This equation updates the belief about the current state after taking an action a and observing an outcome o. The new belief $b'(s')$ is proportional to the likelihood of the observation o given that we end up in the state s', times the sum of the probabilities of reaching s' from all possible states s under an action a, weighted by the current belief about being in the state s.

D. SOLVER CHOICE:

For this problem, a Point-Based Value Iteration (PBVI) algorithm [61], [62] is employed as the solver due to its efficiency and compatibility with problems possessing small, finite discrete state and action spaces. The PBVI solver iteratively optimizes the value function, updating the maximum expected reward for each state-action pair over a number of iterations. The resulting policy, which assigns actions to states, is extracted from this optimal value function. Equation 15 shows how the PBVI works:

$$V_{n+1}(b) = \max_{a \in A} \left[R(b, a) + \gamma \sum_{o \in \mathcal{O}} P(o|b, a) \max_{\alpha \in \Gamma_n} \sum_{s \in \mathcal{S}} \alpha(s) b'(s) \right] \tag{15}$$

In this equation, $V_{n+1}(b)$ represents the value of belief state b at the $n+1$ iteration. $R(b, a)$ is the expected immediate reward for taking an action a in belief state b. In addition, $\alpha(s)$ represents the value of state s for α-vector (defined below). Finally, the $max_{\alpha \in \Gamma_n}$ operation selects the α-vector that yields the highest value for the updated belief state b'.

The aim of PBVI is to find an approximate solution of the POMDP by computing a set of α-vectors. Each α-vector corresponds to a specific action and provides a mapping from the state space to real numbers. In each iteration, the α-vectors are updated according to the equation 15 to improve the value function approximation. The algorithm continues until a termination condition is met, such as a maximum number of iterations or a minimal improvement threshold. In the simulation established in this paper, the condition is related to the maximum number of iterations.

E. VARIABLES INITIALIZATION

Before the simulation is run, all necessary variables associated with the states, actions, and policy are initialized. Initial settings for the train's position, speed, and distance from the obstacle are also established. As the simulation progresses, the position and speed are continuously updated according to

TABLE 1. Variables initialization.

Variable	Initial Value	Unit
Initial train speed	40	$m.s^{-1}$
Initial train position	0	m
Nominal braking distance (α_1)	300	m
Emergency braking distance (α_2)	100	m
Time sample	0.1	s
Rewards $[r_{s_1}, r_{s_2}, r_{s_3}, r_{s_4}]$	$[10, -10, -100, -1000]$	-
Actions forces $[a_1, a_2, a_3]$	$[0, -1, -3]$	$m.s^{-2}$
Discount factor (γ)	0.95	-

the chosen action and the train's current state. These initial values provide a baseline from which the train learns to make optimal decisions (see Table 1).

F. RISK FORMULATION

Once the environment is perceived, the next step is the risk estimation. Here, possible scenarios that can lead to unsafe conditions/collisions are identified, and their probability is estimated based on current and predicted states. This involves the identification of potential hazards, assessment of their possible impact, and the calculation of the risk associated with each hazard. To this end, the risk is calculated in two manners, as described in the following equations:

$$R_1 = 1 - \frac{1}{1 + \exp(-5.\frac{d_o}{\alpha_1})} \tag{16}$$

$$R_2 = \frac{\alpha_1 - d_o}{\alpha_1 - \alpha_2} \tag{17}$$

Equation 16 utilizes a logistic function to present the scenario where risk is relatively low when the train is far from the obstacle ($d_o > \alpha_1$). The use of the logistic function offers a smooth and sigmoidal transition from a low-risk state to a high-risk state. This feature is ideal for representing scenarios where risk is initially low but increases as the train approaches the obstacle, and eventually saturates as the obstacle gets very close. Additionally, this characteristic caters to the fact that when the obstacle is far enough, the train has enough time to react, and the risk is low. On the other hand, when the obstacle is very close ($d_o < \alpha_2$) the train could have already engaged its emergency braking, implying that it has already acknowledged the risk and is attempting to mitigate it.

Equation 17 linearly increases the risk as the train gets closer to the obstacle, from the nominal braking distance (α_1) to the emergency braking distance (α_2). This is logical as when the train is within its nominal braking distance, it should ideally start decelerating to avoid a collision, and failure to do so progressively increases the risk. The risk reaches its peak when the train is at its emergency braking distance, signifying that if the train does not stop immediately, the collision is inevitable.

In summary, both equations are established as a probability ($R_1, R_2 \in [0, 1]^2$) to collectively encapsulate the two critical regions of autonomous train operations from a safety perspective: the proactive safety measures (equation 16) and the reactive safety measures (equation 17).

G. RESULTS

The following figures illustrate the system's performance in a dynamic railway environment, providing valuable insights into its ability to detect and respond to obstacles, estimate risk levels, and ensure safe and efficient operations. In concluding our discussion on the simulation setups, it is important to note that by presenting two distinct scenarios, we demonstrate the inherent advantages of our approach in terms of adaptability and the ease with which new elements or factors can be integrated. The original scenario establishes a baseline, while the enhanced simulation scenario takes a leap forward by incorporating dynamic elements such as obstacle velocities and behaviors.

1) ACTUAL STATE, PERCEIVED STATE, AND CHOSEN ACTION

Figure 7a shows the evolution of the actual state (*in blue color*), perceived state (*in red color*), and the chosen action (*in green color*) over time. The actual state represents the ground truth state of the train, while the perceived state is based on the observations made by the train's sensors. The chosen action is the decision made by the POMDP model based on the perceived state. The plot provides valuable insights into how the perception process impacts decision-making, and it showcases the effectiveness of the model in adapting to the dynamic environment. Moreover, the x-axis in the figure represents the different time steps during the simulation, capturing the sequential evolution of the system's decision-making process. On the y-axis (*on the left*), the values s_1, s_2, s_3, and s_4 correspond to the different states the system can be in. On the other hand, the y-axis (*on the right*) represents also the available actions that the system can take in response to its perceived state. These actions are depicted as a_1, a_2, and a_3.

The perceived state follows the trajectory of the actual state, underscoring the system's ability to accurately perceive its environment. However, some occasional divergences between the two trajectories (perceived and actual state) are present at specific time steps. These divergences are interpreted as false positives (perceiving an obstacle that is not present/false alert) and false negatives (falling to detect an obstacle/missed detection).

Similarly, Figure 8a provides a visualization of the autonomous train's state transitions alongside the corresponding actions taken over the simulation period. The graph displays perceived states in red, actual states in blue, and chosen actions are highlighted in green for clear differentiation and easy interpretation. The plot shows the model's responsiveness to changes in risk levels, transitioning to more conservative actions as the perceived risk increases (i.e., state s_4). Notably, the shift from s_1 to s_4 prompts an immediate action change to a_3, demonstrating the system's capacity for rapid reaction to imminent collision risks.

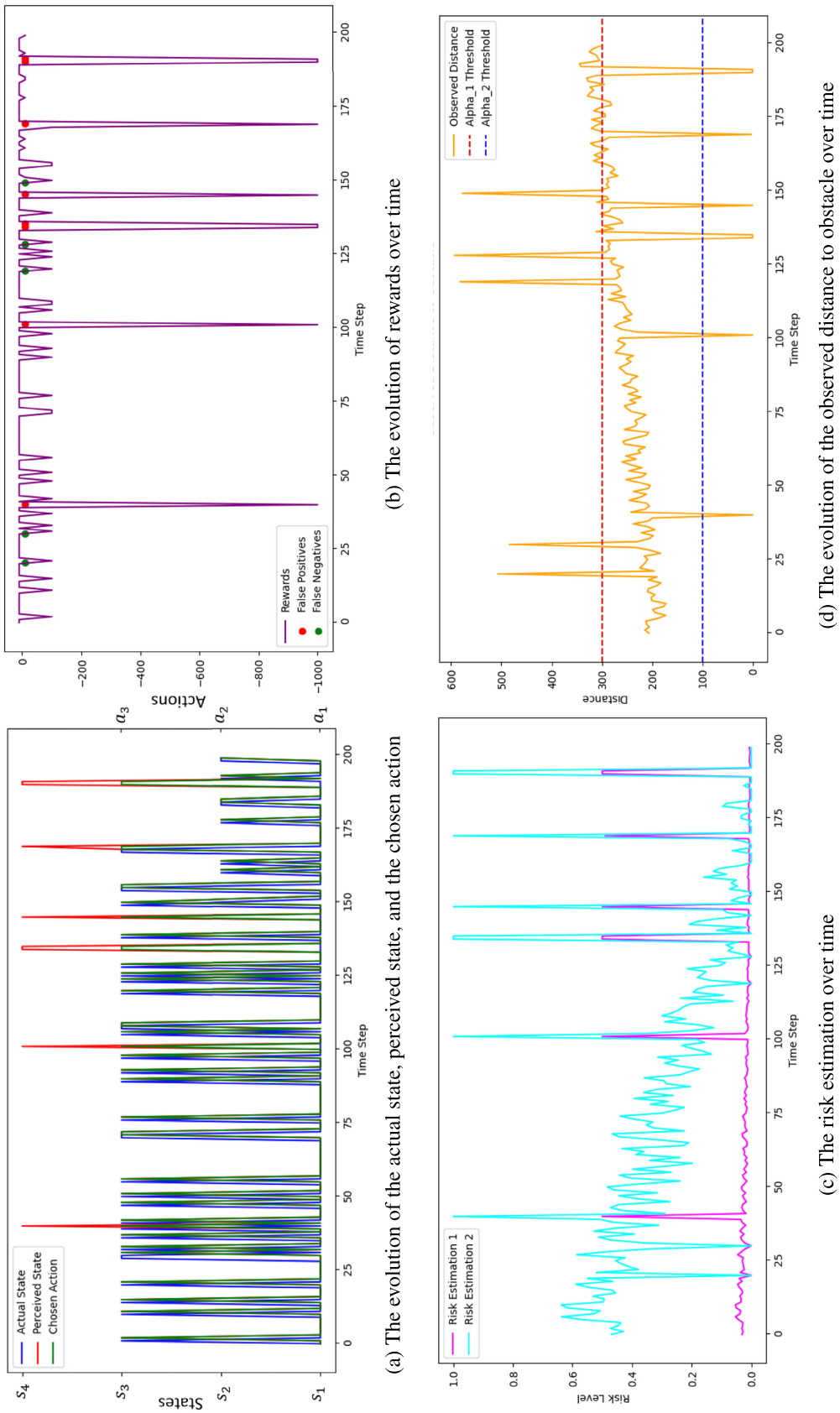

(a) The evolution of the actual state, perceived state, and the chosen action

(b) The evolution of rewards over time

(c) The risk estimation over time

(d) The evolution of the observed distance to obstacle over time

FIGURE 7. Simulation results: setup 1.

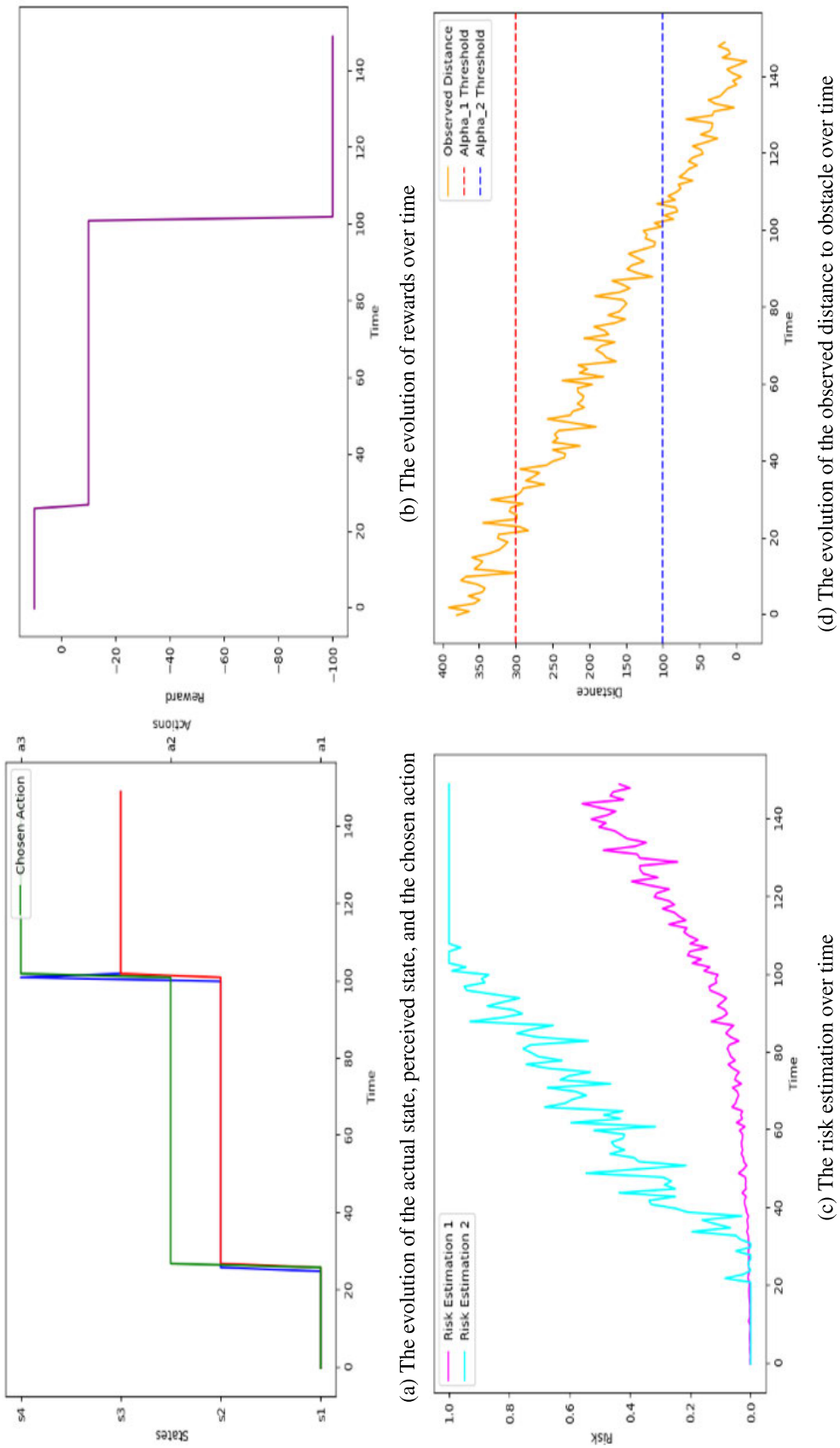

(a) The evolution of the actual state, perceived state, and the chosen action

(b) The evolution of rewards over time

(c) The risk estimation over time

(d) The evolution of the observed distance to obstacle over time

FIGURE 8. Simulation results: setup 2.

2) REWARDS OVER TIME

Figure 7b displays the immediate rewards (and penalties) obtained by the system over time. The rewards are directly linked to the perceived state and the chosen action. Positive rewards indicate safety (*Safe* state), while negative rewards represent potential risks (*ObstacleDetected*, *AboutToCrash*, and *Crash states*). The scatter plots in the figure also highlight false positives (*in green points*) and false negatives (*in red points*) in the decision-making process, showing instances where the model's perception deviates from the actual state. Notable false positives occur at times 40, 101, 134, 135, 145, 169, 190, 191, while false negatives occur at times 20, 30, 119, 149.

Correspondingly, Figure 8b shows the dynamics of the rewards function for the second setup of simulation. The figure clearly denotes the penalty incurred as the system approaches a high-risk state, highlighting the impact of strategic decision-making on the train's overall safety. In the rewards function of the second simulation setup, the concentration is oriented towards the model's ability to integrate dynamic properties of obstacles, such as their velocities and nature. As such, the delineation of false positives and negatives was deemed less pertinent for this particular analysis, given that the primary interest was to observe how the integration of obstacle dynamics affects the overall reward structure and safety performance of the autonomous system.

3) RISK ESTIMATION OVER TIME

Figure 7c illustrates two risk estimation methods: *risk estimation 1* (equation 16) and *risk estimation 2* (equation 17) employed in the model. These estimations assess the risk level associated with the observed distance to the obstacle. Higher risk values indicate a higher likelihood of collision. The plot enables a comprehensive understanding of the risk assessment process and its role in determining appropriate actions.

Risk estimation 1 (depicted in *magenta color*) mainly describes low-risk scenarios across most states (i.e., states s_1, s_2 and s_3, except for the *Crash* state (i.e., state s_4), where risk is high. This approach seems cautious, as it maintains a conservative risk assessment. In contrast, *risk estimation 2* (illustrated in *cyan color*) describes a more dynamic risk evaluation. As the model navigates from the *Safe* state to *AboutToCrash* state, risk steadily increases, reaching approximately 0.5, indicating a heightened state of caution. However, once the model enters the *Crash* state, risk reaches its maximum value of 1, underscoring the severe consequences of this state. These differing risk estimation strategies shed light on the adaptability of the model, reveal the ability to respond to different levels of risk, and provide valuable insights into the decision-making process.

Equally, Figure 8c illustrates the fluctuating risk levels as perceived by each method over time, with *Risk Estimation 1* and *Risk Estimation 2* plotted on the same graph for direct comparison. The divergence two methods underscores the variability in risk perception and the importance of selecting a robust model that accurately reflects the operational condition's inherent uncertainties.

4) OBSERVED DISTANCE TO OBSTACLE

Figure 7d depicts the observed distance to the obstacle over time. It tracks how the perceived distance fluctuates as the train's sensors detect and interact with the environment. The red and blue dashed lines represent the thresholds for the nominal and emergency braking distances (α_1 and α_2, respectively). When the observed distance crosses these thresholds, the model may initiate braking actions accordingly to prevent potential collisions.

On the other hand, Figure 8d showcases the observed distance to the nearest obstacle throughout the simulation timeline. In this second simulation setup, the model considers multiple obstacles, both static and dynamic, and calculates the distance to the nearest obstacle (i.e., the *distance to obstacle* variable). The plot is a testament to the system's ability to maintain situational awareness and adapt its responses based on real-time assessments.

The results of the simulation demonstrate the effectiveness of the proposed risk-based POMDP process for the autonomous train anti-collision function. The results show that the proposed model is able to provide a safe and efficient solution for the anti-collision function, which takes into account the uncertainties related to the train's state and its perception of the environment. Moreover, this highlights the potential of the proposed process to be applied to real-world scenarios and provides a basis for further research to improve and extend the process to handle more complex environments. Finally, the dual-scenario structure not only showcases the robustness of our model but also represents the initial steps towards a more generic and comprehensive approach. In future iterations, the model could evolve to include additional complexities such as the precise dimensions of obstacles, their predicted trajectories, and other environmental factors. These advancements will allow for a more detailed and far-reaching application of the POMDP model, pushing the boundaries of autonomous train safety and operational efficiency.

VI. CONCLUSION AND PERSPECTIVES

In this paper, we proposed a risk-based decision-making approach for autonomous trains, leveraging the capabilities of Partially Observable Markov Decision Processes (POMDPs) to facilitate effective and real-time environmental monitoring of trains. The core contribution of this study lies in the ongoing monitoring and risk estimation, which is crucial for ensuring the safe operation of autonomous trains. This approach integrates dynamic risk assessment into the core of the decision-making process, enabling the train to proactively manage potential collision hazards. It effectively addresses uncertainties in both the train's operational state and its interaction with the environment. By doing so, the approach enhances the autonomous train's ability to make informed and safe decisions.

REFERENCES

[1] D. Trentesaux, R. Dahyot, A. Ouedraogo, D. Arenas, S. Lefebvre, W. Schön, B. Lussier, and H. Chéritel, "The autonomous train," in *Proc. 13th Annu. Conf. Syst. Syst. Eng. (SoSE)*, Jun. 2018, pp. 514–520.

[2] R. Lagay and G. M. Adell, "The autonomous train: A game changer for the railways industry," in *Proc. 16th Int. Conf. Intell. Transp. Syst. Telecommun. (ITST)*, Oct. 2018, pp. 1–5.

[3] F. Boudardara, A. Boussif, P.-J. Meyer, and M. Ghazel, "Interval weight-based abstraction for neural network verification," in *Computer Safety, Reliability, and Security. SAFECOMP Workshops*. Springer, 2022, pp. 330–342.

[4] F. Boudardara, A. Boussif, P.-J. Meyer, and M. Ghazel, "INNAbstract: An INN-based abstraction method for large-scale neural network verification," *IEEE Trans. Neural Netw. Learn. Syst.*, Oct. 2023.

[5] F. Boudardara, A. Boussif, P.-J. Meyer, and M. Ghazel, "A review of abstraction methods towards verifying neural networks," *ACM Trans. Embedded Comput. Syst.*, vol. 22, pp. 1–17, Jul. 2023.

[6] A. Mahtani, N. Chouchani, M. Herbreteau, and D. Rafin, "Enhancing autonomous train safety through a priori-map based perception," in *Proc. 4th Int. Conf. Rel., Saf., Secur. Railway Syst. (RSSRail)*, Paris, France, Jun. 2022, pp. 115–129.

[7] A. Boussik, P. Antoine, W. B. Messaoud, A. Taleb-Ahmed, S. Niar, A. Bekrar, and D. Trentesaux, "Vision-based railway track extraction and obstacle detection using deep learning for autonomous train," in *Proc. 2nd Int. Workshop Artif. Intell. RAILwayS (AIRAILS)*, 2021, p. 190.

[8] M. Chelouati, A. Boussif, J. Beugin, and E.-M. El-Koursi, "A framework for risk-awareness and dynamic risk assessment for autonomous trains," in *Proc. 32nd Eur. Saf. Rel. Conf. (ESREL)*, Sep. 2022, pp. 2128–2135.

[9] A. Lemonnier, S. Adelé, and C. Dionisio, "The determinants of acceptability and behavioural intention of automated vehicles—A review," *Le Travail Humain*, vol. 83, no. 4, pp. 297–342, Nov. 2020.

[10] Y. Alsaba, M. Berbineau, I. Dayoub, E. Masson, G. M. Adell, and E. Robert, "5G for remote driving of trains," in *Proc. Int. Workshop Commun. Technol. Vehicles*, 2020, pp. 137–147.

[11] *Railway applications - The Specification and Demonstration of Reliability, Availability, Maintainability and Safety (RAMS)*, Standard EN50126, 2017.

[12] M. Chelouati, A. Boussif, J. Beugin, and E.-M. El Koursi, "Graphical safety assurance case using goal structuring notation (GSN)—Challenges, opportunities and a framework for autonomous trains," *Rel. Eng. Syst. Saf.*, vol. 230, Feb. 2023, Art. no. 108933.

[13] A. Boussif, A. Tonk, J. Beugin, and S. Collart Dutilleul, "Operational risk assessment of railway remote driving system," *Saf. Rel.*, pp. 1–22, May 2023.

[14] A. Tonk, M. Chelouati, A. Boussif, J. Beugin, and M. El Koursi, "A safety assurance methodology for autonomous trains," *Transp. Res. Arena*, vol. 72, pp. 3016–3023, Jun. 2022.

[15] D. Heß, S. Lapoehn, F. Utesch, M. Fischer, J. Schindler, T. Hesse, and F. Köster, "Contributions of the EU projects UnCoVerCPS and enable-S3 to highly automated driving in conflict situations," in *Proc. Annu. Conf. Amer. Assoc. Electrodiagnostic Technol.*, 2019, pp. 1–25.

[16] A. Bondavalli, A. Ceccarelli, J. Grønbæk, D. Iovino, L. Kárná, Š. Klapka, T. K. Madsen, M. Magyar, I. Majzik, and A. Salzo, "Design and evaluation of a safe driver machine interface," *Int. J. Performability Eng.*, vol. 5, no. 2, pp. 153–166, 2009.

[17] A. Sutton, "The development of rail vehicle crashworthiness," *Proc. Inst. Mech. Eng., F, J. Rail Rapid Transit*, vol. 216, no. 2, pp. 97–108, Mar. 2002.

[18] C. G. Burns, L. Oliveira, P. Thomas, S. Iyer, and S. Birrell, "Pedestrian decision-making responses to external human-machine interface designs for autonomous vehicles," in *Proc. IEEE Intell. Vehicles Symp. (IV)*, Jun. 2019, pp. 70–75.

[19] T. Parhizkar, I. B. Utne, J.-E. Vinnem, and T. Parhizkar, *Online Probabilistic Risk Assessment of Complex Marine Systems: Principles, Modelling and Applications* (Springer Series in Reliability Engineering), 1st ed. Cham, Switzerland: Springer, 2021.

[20] F. Khan, S. J. Hashemi, N. Paltrinieri, P. Amyotte, V. Cozzani, and G. Reniers, "Dynamic risk management: A contemporary approach to process safety management," *Current Opinion Chem. Eng.*, vol. 14, pp. 9–17, Nov. 2016.

[21] O. Gebauer, W. Pree, and B. Stadlmann, "Autonomously driving trains on open tracks—Concepts, system architecture and implementation aspects," *Inf. Technol.*, vol. 54, no. 6, pp. 266–279, Nov. 2012.

[22] S. Chouhan et al., "Railway anti-collision system using DSLR sensor," *Int. J. Eng. Sci. Res.*, vol. 3, pp. 1199–1202, Mar. 2014.

[23] P. Richard, A. Boussif, and C. Paglia, "Rule-based and managed safety: A challenge for railway autonomous driving systems," in *Proc. 31st Eur. Saf. Rel. Conf. (ESREL)*, Sep. 2021, pp. 2363–2369.

[24] F. Rosique, P. J. Navarro, C. Fernández, and A. Padilla, "A systematic review of perception system and simulators for autonomous vehicles research," *Sensors*, vol. 19, no. 3, p. 648, Feb. 2019.

[25] G. S. Nair and C. R. Bhat, "Sharing the road with autonomous vehicles: Perceived safety and regulatory preferences," *Transp. Res. C, Emerg. Technol.*, vol. 122, Jan. 2021, Art. no. 102885.

[26] *Operational Design Domain (ODD) Taxonomy for an Automated Driving System (ADS)*, Standard PAS 1883:2020, European PAS 1883, 2020.

[27] S. Gupta and I. Snigdh, "Multi-sensor fusion in autonomous heavy vehicles," in *Autonomous and Connected Heavy Vehicle Technology*. Amsterdam, The Netherlands: Elsevier, 2022, pp. 375–389.

[28] H. Shao, L. Wang, R. Chen, H. Li, and Y. Liu, "Safety-enhanced autonomous driving using interpretable sensor fusion transformer," in *Proc. Conf. Robot Learn.*, 2023, pp. 726–737.

[29] J. Molloy and J. McDermid, "Safety assessment for autonomous system perception capabilities," 2022, *arXiv:2208.08237*.

[30] Z. Gu, L. Gao, H. Ma, S. E. Li, S. Zheng, W. Jing, and J. Chen, "Safe-state enhancement method for autonomous driving via direct hierarchical reinforcement learning," *IEEE Trans. Intell. Transp. Syst.*, vol. 24, no. 9, Sep. 2023.

[31] K. Yang, B. Li, W. Shao, X. Tang, X. Liu, and H. Wang, "Prediction failure risk-aware decision-making for autonomous vehicles on signalized intersections," *IEEE Trans. Intell. Transp. Syst.*, vol. 24, no. 11, pp. 12806–12820, Nov. 2023.

[32] K. Yang, X. Tang, J. Li, H. Wang, G. Zhong, J. Chen, and D. Cao, "Uncertainties in onboard algorithms for autonomous vehicles: Challenges, mitigation, and perspectives," *IEEE Trans. Intell. Transp. Syst.*, pp. 1–25, 2023.

[33] Y. Zhang, A. Carballo, H. Yang, and K. Takeda, "Perception and sensing for autonomous vehicles under adverse weather conditions: A survey," *ISPRS J. Photogramm. Remote Sens.*, vol. 196, pp. 146–177, Feb. 2023.

[34] W. Lobato, P. Mendes, D. Rosário, E. Cerqueira, and L. A. Villas, "Redundancy mitigation mechanism for collective perception in connected and autonomous vehicles," *Future Internet*, vol. 15, no. 2, p. 41, Jan. 2023.

[35] T. Johansen, S. Blindheim, T. R. Torben, I. B. Utne, T. A. Johansen, and A. J. Sørensen, "Development and testing of a risk-based control system for autonomous ships," *Rel. Eng. Syst. Saf.*, vol. 234, Jun. 2023, Art. no. 109195.

[36] V. Bolbot, G. Theotokatos, L. Wennersberg, J. Faivre, D. Vassalos, E. Boulougouris, Ø. J. Rødseth, P. Andersen, A.-S. Pauwelyn, and A. Van Coillie, "A novel risk assessment process: Application to an autonomous inland waterways ship," *Proc. Inst. Mech. Eng., O, J. Risk Rel.*, vol. 237, no. 2, pp. 436–458, Apr. 2023.

[37] A. Sarker, P. Fisher, J. E. Gaudio, and A. M. Annaswamy, "Accurate parameter estimation for safety-critical systems with unmodeled dynamics," *Artif. Intell.*, vol. 316, Mar. 2023, Art. no. 103857.

[38] J. Hegde, I. B. Utne, I. Schjølberg, and B. Thorkildsen, "A Bayesian approach to risk modeling of autonomous subsea intervention operations," *Rel. Eng. Syst. Saf.*, vol. 175, pp. 142–159, Jul. 2018.

[39] J. Kim, X. Zhao, A. U. A. Shah, and H. G. Kang, "System risk quantification and decision making support using functional modeling and dynamic Bayesian network," *Rel. Eng. Syst. Saf.*, vol. 215, Nov. 2021, Art. no. 107880.

[40] M. M. Abaei, R. Hekkenberg, and A. BahooToroody, "A multinomial process tree for reliability assessment of machinery in autonomous ships," *Rel. Eng. Syst. Saf.*, vol. 210, Jun. 2021, Art. no. 107484.

[41] B. R. Kiran, I. Sobh, V. Talpaert, P. Mannion, A. A. A. Sallab, S. Yogamani, and P. Pérez, "Deep reinforcement learning for autonomous driving: A survey," *IEEE Trans. Intell. Transp. Syst.*, vol. 23, no. 6, pp. 4909–4926, Jun. 2022.

[42] P. G. Morato, C. P. Andriotis, K. G. Papakonstantinou, and P. Rigo, "Inference and dynamic decision-making for deteriorating systems with probabilistic dependencies through Bayesian networks and deep reinforcement learning," *Rel. Eng. Syst. Saf.*, vol. 235, Jul. 2023, Art. no. 109144.

[43] A. Plissonneau, D. Trentesaux, W. Ben-Messaoud, and A. Bekrar, "AI-based speed control models for the autonomous train: A literature review," in *Proc. 3rd Int. Conf. Transp. Smart Technol. (TST)*, May 2021, pp. 9–15.

[44] D. Q. Tran and S.-H. Bae, "Improved responsibility-sensitive safety algorithm through a partially observable Markov decision process framework for automated driving behavior at non-signalized intersection," *Int. J. Automot. Technol.*, vol. 22, no. 2, pp. 301–314, Apr. 2021.

[45] P. Pouya and A. M. Madni, "Expandable-partially observable Markov decision-process framework for modeling and analysis of autonomous vehicle behavior," *IEEE Syst. J.*, vol. 15, no. 3, pp. 3714–3725, Sep. 2021.

[46] R. Wisniewski and M. L. Bujorianu, "Probabilistic safety guarantees for Markov decision processes," *IEEE Trans. Autom. Control*, vol. 68, no. 12, Dec. 2023.

[47] R. G. Maidana, T. Parhizkar, A. Gomola, I. B. Utne, and A. Mosleh, "Supervised dynamic probabilistic risk assessment: Review and comparison of methods," *Rel. Eng. Syst. Saf.*, vol. 230, Feb. 2023, Art. no. 108889.

[48] X. Xu, J. Peng, R. Zhang, B. Chen, F. Zhou, Y. Yang, K. Gao, and Z. Huang, "Adaptive model predictive control for cruise control of high-speed trains with time-varying parameters," *J. Adv. Transp.*, vol. 2019, pp. 1–11, May 2019.

[49] S. Ragi and E. K. P. Chong, "UAV path planning in a dynamic environment via partially observable Markov decision process," *IEEE Trans. Aerosp. Electron. Syst.*, vol. 49, no. 4, pp. 2397–2412, Oct. 2013.

[50] K. A. Svendsen and M. L. Seto, "Partially observable Markov decision processes for fault management in autonomous underwater vehicles," in *Proc. IEEE Can. Conf. Electr. Comput. Eng. (CCECE)*, Aug. 2020, pp. 1–7.

[51] M. Lauri, D. Hsu, and J. Pajarinen, "Partially observable Markov decision processes in robotics: A survey," *IEEE Trans. Robot.*, vol. 39, no. 1, pp. 21–40, Feb. 2023.

[52] S. Ross, J. Pineau, S. Paquet, and B. Chaib-draa, "Online planning algorithms for POMDPs," *J. Artif. Intell. Res.*, vol. 32, pp. 663–704, Jul. 2008.

[53] D. Silver and J. Veness, "Monte–Carlo planning in large POMDPs," in *Proc. Adv. Neural Inf. Process. Syst. (NIPS)*, vol. 23, 2010, pp. 2164–2172.

[54] A. Somani, N. Ye, D. Hsu, and W. S. Lee, "DESPOT: Online POMDP planning with regularization," in *Proc. Adv. Neural Inf. Process. Syst.*, vol. 26, 2013, pp. 231–266.

[55] D. Klimenko, J. Song, and H. Kurniawati, "TAPIR: A software toolkit for approximating and adapting POMDP solutions online," in *Proc. Australas. Conf. Robot. Autom.*, Melbourne, VIC, Australia, vol. 24, 2014, pp. 1–9.

[56] Z. Sunberg and M. J. Kochenderfer, "POMCPOW: An online algorithm for POMDPs with continuous state, action, and observation spaces," in *Proc. 28th Int. Conf. Automated Planning Scheduling*, 2017, pp. 259–263.

[57] X. Xiang and S. Foo, "Recent advances in deep reinforcement learning applications for solving partially observable Markov decision processes (POMDP) problems: Part 1—Fundamentals and applications in games, robotics and natural language processing," *Mach. Learn. Knowl. Extraction*, vol. 3, no. 3, pp. 554–581, Jul. 2021.

[58] H. Kumamoto and E. J. Henley, *Probabilistic Risk Assessment and Management for Engineers and Scientists*. Piscataway, NJ, USA: IEEE Press, 1996.

[59] S. Temizer, M. Kochenderfer, L. Kaelbling, T. Lozano-Perez, and J. Kuchar, "Collision avoidance for unmanned aircraft using Markov decision processes," in *Proc. AIAA Guid., Navigat., Control Conf.*, Aug. 2010, p. 8040.

[60] E. Leurent. (2018). *A Survey of State-Action Representations for Autonomous Driving*. [Online]. Available: https://hal.archives-ouvertes.fr/hal-01908175/

[61] J. Pineau, G. Gordon, and S. Thrun, "Point-based value iteration: An anytime algorithm for POMDPs," in *Proc. 18th Int. Joint Conf. Artif. Intell. (IJCAI)*, vol. 3, 2003, pp. 1025–1032.

[62] M. T. J. Spaan and N. Vlassis, "Perseus: Randomized point-based value iteration for POMDPs," *J. Artif. Intell. Res.*, vol. 24, pp. 195–220, Aug. 2005.

MOHAMMED CHELOUATI received the Engineering degree and master's degree in maintenance, operational management, and risk management, and in complex systems engineering from the Polytech Nancy and Lorraine University, Nancy, in 2020. He is currently pursuing the joint Ph.D. degree in railways safety with Gustave Eiffel University, Villeneuve d'Ascq, Lille, France, and the Technological Research Institute Railenium, Valenciennces, France.

His Ph.D. degree deal with safety assurance of the autonomous train. He is the author of four articles. His research interests include railway safety, more specifically, and the safety of autonomous trains. He has participated in Train Autonome—Service Voyageur (TASV) Project, which is a part of Tech4Rail Program both initiated by the Direction of Railway Systems (SNCF) and PRISMA in the part of autonomous vehicle's safety.

ABDERRAOUF BOUSSIF received the B.Eng. degree in system control engineering from the Polytechnic High School, Algiers, Algeria, in 2012, the master's degree in complex systems engineering from École Normale Supérieure de Cachan, Paris, in 2013, and the Ph.D. degree in safety system engineering from the University of Lille, France, in 2016. He is currently a Research Associate with the Evaluation and Safety of Automated Transport Systems Research Team (COSYS/ESTAS), Gustave Eiffel University. His research interests include the dependability and safety assurance of railway systems, formal methods, MBSA, and AI safety, with a particular emphasis on railway control command and signaling systems.

JULIE BEUGIN received the Engineering degree from INSA Hauts-de-France (National Institute of Applied Sciences), in 2002, the master's degree in automation engineering from the Polytechnic University of Hauts-de-France, in 2002, and the Ph.D. degree in automation and computing sciences, in 2006.

Since 2007, she has been with Gustave Eiffel University as a Researcher. Her research interests in the ESTAS Laboratory deals with dependability and safety evaluation of complex guided transportation systems. Part of her activities addresses RAMS demonstration issues of GNSS-based solutions embedded in train control applications. She has participated in the GaLoROI, ERSAT-GGC, STARS, PERFORMINGRAIL, and X2-Rail European projects. She has secondment agreements with Railenium to participate in projects in her research fields, especially the Autonomous Train—Passengers Service Project, and also with Certifer to realize ISA missions.

EL-MILOUDI EL-KOURSI received the master's degree in electronic and the Ph.D. degree in computer dependability sciences from the University of Lille, France, in 1982 and 1985, respectively. He is currently a Research Director with the Evaluation and Safety of Automated Transport Systems Research Team (COSYS/ESTAS), Gustave Eiffel University. He has 25 years of experience in performing assessment and certification of safety-related rail and associated systems. In recent years, he has been involved in various European projects. He was also the Leader of the European FP5 Safety Management and Interoperability Thematic Network and the Leader of the sixth pole on "safety and security" within the FP6 European Rail Research Network of Excellence. He has organized several conferences and workshops on railway issues and he is a reviewer for several international journals in the transportation and safety domains.